PPARγ is a Major Driver of the Accumulation and Phenotype of Adipose-Tissue \(T_{reg}\) Cells

Published in final edited form as:
Nature. 2012 June 28; 486(7404): 549–553. doi:10.1038/nature11132.

PPARγ is a major driver of the accumulation and phenotype of adipose-tissue T_{reg} cells

Daniela Cipolletta[1], **Markus Feuerer**[1,2], **Amy Li**[1], **Nozomu Kamei**[3,4], **Jongsoon Lee**[3], **Steven E. Shoelson**[3], **Christophe Benoist**[1,*], and **Diane Mathis**[1,*]

[1]Division of Immunology, Department of Microbiology and Immunobiology, Harvard Medical School, Boston, MA 02115

[3]Joslin Diabetes Center and Department of Medicine, Harvard Medical School, Boston, MA 02215

Abstract

Obesity and type-2 diabetes (T2D) have increased dramatically over the past several decades, in parallel. One of the major links between these two disorders is chronic, low-grade inflammation [1]. Prolonged nutrient excess promotes the accumulation and activation of leukocytes in visceral adipose tissue (VAT) and ultimately other tissues, which provokes metabolic abnormalities such as insulin resistance, T2D and fatty-liver disease. While invasion of VAT by pro-inflammatory macrophages is considered to be a key event driving adipose-tissue inflammation and insulin resistance, little is known about the roles of other immune-system cell-types in these processes. Recently, a unique population of VAT-resident regulatory T cells (T_{regs}) was implicated in control of the inflammatory state of adipose tissue and, thereby, insulin sensitivity [2]. We have identified peroxisome proliferator-activated receptor gamma (PPARγ), the "master-regulator" of adipocyte differentiation, as a critical molecular orchestrator of VAT T_{reg} accumulation, phenotype and function. Unexpectedly, PPARγ expression by VAT T_{regs} was necessary for complete restoration of insulin sensitivity in obese mice by the thiazolidinedione (TZD) drug, pioglitazone (Pio). These findings suggest a previously unknown cellular mechanism for this important class of T2D drugs, and provide proof-of-principle that discrete populations of T_{regs} with unique functions can be precisely targeted to therapeutic ends.

Keywords

regulatory T cell; adipose tissue; obesity; type-2 diabetes; nuclear receptor; TZD drug

A unique population of $Foxp3^+CD4^+$ T_{regs} was recently found in the VAT of normal individuals [2], as a much higher fraction of the $CD4^+$ T cell compartment than that usually observed in lymphoid or other non-lymphoid tissues. VAT T_{regs} had a phenotype readily distinguishable from that of their counterparts in the spleen and lymph nodes (LNs), including a distinct gene-expression profile, T cell receptor repertoire, and pattern of chemokine and chemokine receptor expression. Adipose-tissue inflammation and both local

[*]Address correspondence to: Diane Mathis, Harvard Medical School, 77 Avenue Louis Pasteur, Boston, MA 02115, cbdm@hms.harvard.edu, Phone: (617) 432-7741, Fax: (617) 432-7744.
[2]**Present address:** German Cancer Research Center (DKFZ), Heidelberg, Germany
[4]**Present address:** University of Tokyo, Tokyo, Japan

Author contributions: All authors designed research; D.C. and A.L. performed research; D.C., S.S., C.B. and D.M. analyzed data; D.C., C.B. and D.M. wrote the paper.

Conflict of interest: D.M., C.B., M.F. and S.S. have a patent pending on fat T_{regs}.

and systemic metabolic indices were improved or worsened by global enrichment or impoverishment, respectively, of T_{regs} [2–4]. However, a lack of appropriate reagents has so far precluded an assessment of the precise role of fat-resident T_{regs}.

The molecules that orchestrate the distinctive properties of VAT T_{regs} are unknown. Comparing the gene-expression profiles of visceral-fat and lymphoid-organ T_{regs}, we were struck by the elevated level of transcripts encoding the nuclear receptor PPARγ in the former (Fig. 1a, Suppl. Fig. S1a). The specificity of this increase was highlighted by a comparison of *Pparg* transcript levels across a large library of microarray data-sets (more than 350) encompassing T cells of diverse subsets, activation statuses and localizations (Fig. 1b). Because of the crucial role of PPARγ in adipocyte differentiation, as well as its anti-inflammatory activities [5], we hypothesized that its expression in VAT T_{regs} might be responsible for at least some of their unique features.

To identify genes whose expression was correlated, either positively or negatively, with that of *Pparg*, we performed a clustering analysis across transcript profiles obtained from VAT and LN T_{regs} of mice differing in their metabolic state: either lean [C57Bl/6 (B6) animals of various ages kept on normal chow (NC)] or obese [B6.*Lep*$^{ob/ob}$ (ob/ob) animals of varying age on NC or B6 animals on a high-fat diet (HFD)] (Suppl. Fig. S1b and c). The set of loci whose expression was co- or anti-correlated with *Pparg* transcript levels encompassed the majority of those most strongly up- (red) or down- (blue) regulated, respectively, in visceral-fat versus lymphoid-tissue T_{regs} [2] (Fig. 1c). The co-clustered transcripts included many that encode chemokines or chemokine receptors involved in leukocyte migration and extravasation (e.g., *Ccr2* and *3*, *Cxcr6*, *Cxcl2* and *3*), several encoding molecules involved in lipid metabolism (e.g., *Pcyt1a*, *Dgat1*), and *Il10* transcripts.

We directly evaluated the role of PPARγ in specifying the VAT T_{reg} phenotype by retrovirally transducing *Foxp3* alone or together with *Pparg* into naïve $CD4^+$ T cells activated *in vitro* with anti-CD3/CD28-coated beads (neither transcription factor being expressed at detectable levels in the host $CD4^+$ T cells). Two isoforms of PPARγ have been described, referred to as PPARγ1 and PPARγ2 [5]; while adipocytes are known to express both of them, the isoform(s) made by T lymphocytes are not well characterized. Feature-level analysis of *Pparg* transcripts, exploiting our existing Affymetrix ST 1.0 microarray data, revealed that mRNAs corresponding to both PPARγ1 and PPARγ2 were expressed by VAT T_{regs}, with predominance of the former (Suppl. Fig. S2a), while the low-level transcripts made by the other T cell populations encoded primarily PPARγ2 (not shown). Therefore, we evaluated each isoform's ability to cooperate with Foxp3 to promote the VAT T_{reg} gene-expression signature. Most transcripts are distributed in a gray cloud along the diagonal in the Fold-change/Fold-change (FC/FC) plot of Fig. 2a, showing that *Pparg1* and *Pparg2* induced the expression of a similar set of genes when co-transduced with *Foxp3*; the slight tilt towards the x-axis indicates that *Pparg1* transduction was a bit more potent. Each isoform promoted expression of the above-discussed *Pparg* co-cluster (red cloud along the diagonal), while only *Pparg1* repressed expression of the bulk of the *Pparg* anti-cluster (blue cloud along the x-axis). Similarly, as illustrated most clearly by the *Pparg+Foxp3* vs *Foxp3*-alone "volcano plots" (Fig. 2b and c), each PPARγ isoform could collaborate with Foxp3 to up-regulate a substantial fraction of the genes characteristic of the VAT T_{reg} up-signature (pink, skewed to the right in panels b and c). However, the corresponding down-signature was partially recapitulated only after *Pparg1+Foxp3* transduction (green, skewed to the left in panel c but not panel d).

Since adequate PPARγ ligand might not be available in this *in vitro* context, we explored the effect of adding a synthetic agonist, the TZD drug, Pio. Twenty-four hours after retroviral infection, double (*Pparg1+Foxp3* or *Pparg2+Foxp3*) or single (*Foxp3*-alone)

transductants were treated with Pio for forty-eight hours. The most striking effect of this agonist, whether in the context of *Pparg1* or *Pparg2*, was the augmentation of a set of "lipid metabolism" genes, some of which were reported to be differentially expressed in VAT vis-á-vis LN T_{regs} in a previous *ex vivo* microarray analysis [2]. This influence was most obvious on FC/FC plots (Fig. 2d and e), which serve to isolate the effect of Pio in the context of each isoform (as aligned towards the x-axis). Up-regulated genes involved in lipid metabolism included those coding for: fatty-acid transporters (*Cd36, Slc27a2*), enzymes involved in fatty-acid synthesis (*Lipe* and *Scd1*), an enzyme essential for fatty-acid oxidation (*Cpt1a*), an enzyme responsible for the synthesis of triglycerides (*Dgat1*), and a lipid-droplet-associated protein *(Plin2*). Similar results were obtained with Rosiglitazone (Rosi), another TZD drug, or with GW1929, a potent non-TZD PPARγ agonist (Suppl. Figs. S2b and c; note change in axis labels vis-á-vis Figs. 2d and e). The fact that PPARγ could cooperate with Foxp3 to impose a VAT T_{reg} phenotype on naïve $CD4^+$ T cells raised the question of whether the two transcription factors interact in some way. Indeed, both PPARγ isoforms were co-immunoprecipitated with Foxp3 in transduced HEK293 cells, arguing that they have the potential to interact, either directly or within a shared complex (Fig. 2f). (Unfortunately, we could not obtain adequate material from *ex vivo* T cells to perform an analogous experiment.)

To assess the importance of PPARγ for the VAT T_{reg} phenotype *in vivo* we abrogated its expression specifically in T_{regs} by crossing a mouse line carrying "floxed" *Pparg* with a line expressing the Cre recombinase under the dictates of *Foxp3* promoter/enhancer elements. The T_{reg} specificity of Cre expression in such mice has been validated in a number of contexts. At 25 weeks, the resulting mutants (T_{reg}-*Pparg* mut) had lower fractions and numbers of VAT T_{regs} than their *Pparg* wild-type (*Pparg* wt) littermates (carrying the *Foxp3-Cre* transgene); in contrast, the representation of T_{regs} in the lymphoid organs of mutants was normal (Fig. 3a). While VAT T_{regs} in wt mice increased >2.5-fold between 15 and 25 weeks to eventually constitute >40% of the $CD4^+$ T cell compartment, this subset remained below ~10% in mutant mice (Suppl. Fig. S3a). The T_{regs} remaining in the VAT (but not those in the spleen) of mutants had a lower mean fluorescence-intensity (MFI) of Foxp3 expression than that of their wt counterparts (Suppl. Fig. S3b). A volcano plot comparing gene expression in VAT T_{regs} from *Pparg* wt and T_{reg}-*Pparg* mut mice revealed the VAT T_{reg} up-signature (pink, skewed to the right) to be under-represented in mutant T cells while, conversely, the down-signature (green, skewed to the left) was over-represented (Fig. 3b). VAT and lymphoid-organ T_{regs} were much more similar in T_{reg}-*Pparg* mut than in *Pparg* wt mice (Suppl. Fig. S3c); this difference reflected alterations at the level of VAT T_{regs} as the absence of PPARγ expression in LN T_{regs} had little impact (Suppl. Fig. 3d). This observation was confirmed at the protein level (Suppl. Fig. S4): down-regulation of CCR2, Gata-3, KLRG1 and CD69 in mutant vis-á-vis wt VAT T_{regs} to resemble the lower levels in lymphoid-tissue T_{regs}; up-regulation of CD103 and CD86 in mutant VAT T_{regs} to approach the higher levels in lymphoid T_{regs}. Thus, PPARγ is an important factor controlling the accumulation and phenotype of T_{regs} residing in adipose tissue.

How did the loss of PPARγ influence the turnover of T_{regs} residing in VAT? Addressing this question was more complex than simply comparing the half-life of VAT T_{regs} in wild-type and mutant mice because the residual T_{regs} in the latter animals are likely to be atypical "survivors" and/or recruits from the lymphoid T_{reg} pool exploiting a niche empty of the usual competitors. So we performed an acute assay, monitoring T_{reg} populations in wt mice over a few days of treatment with the irreversible PPARγ inhibitor, GW9662 (Suppl. Fig. S5a). There were no significant differences in either VAT or spleen T_{reg} fraction or numbers in the drug- vs vehicle-treated animals (Suppl. Fig. S5b and c). However, there was a progressive decline in the fraction of Gata-3^+ T_{regs} in VAT (but not in spleen) and a parallel decrease in the Gata-3 MFI (Suppl. Fig. S5d and e). Gata-3 is a transcription factor highly

over-represented in VAT versus lymphoid-tissue T_{regs}, and is down-regulated in the absence of PPARγ (Suppl. Fig. S4). Altogether, our data indicate that PPARγ may control both the establishment and maintenance of the VAT T_{reg} phenotype.

Secondarily, the T_{reg}-*Pparg* mut mice had fractional and numerical increases in some, but not all, adipose-tissue monocyte/macrophage subsets: pro-inflammatory $CD11b^+CD11c^+F4/80^+$ macrophages (Suppl. Fig. S6a and S6c) and pro-inflammatory $CD11b^+Ly6c^{hi}$ monocytes (Suppl. Fig. S6b, left and S6d, left), but not $CD11b^+Ly6c^{low}$ monocytes (Suppl. Fig. S6b, right and S6d, right), considered to be anti-inflammatory. There were no changes in fractions or numbers of $CD8^+$ T or B cells in VAT of mutant mice (Suppl. Fig. S6e–h).

Pio is a well-known insulin-sensitizing agent that improves metabolic indices in obese mice and humans. Given its ability to enhance the unique fat T_{reg} signature in cultured cells (Fig 2d and e), we wondered how this drug might impact VAT T_{regs} in obese (HFD-fed) mice. There was an impressive enrichment of the fraction and number of T_{regs} in epididymal adipose tissue of animals treated with Pio (Figs. 4a and Suppl. Fig. S7a), which was a specific effect, not seen in the spleen, subcutaneous fat, peri-renal fat or liver (Figs. 4a and Suppl. Fig. S7b). There were also marked phenotypic changes in the epididymal fat T_{reg} population of Pio-treated *vis-á-vis* untreated obese mice: an overall shift of the gene-expression profile towards that typical of VAT T_{regs} (Fig. 4b); an increase in the Foxp3 MFI (Suppl. Fig. S7c); a PPARγ-dependent enrichment of cells expressing Gata-3 (Suppl. Fig. S7d); and enhanced cell-surface display of the lipid scavenger, CD36 (Fig. 4c). As PPARγ ligands are known to stimulate oxidized low-density lipoprotein (oxLDL) uptake by augmenting levels of CD36 on the surface of macrophages [6], we stained T_{regs} with Nile red, a dye that selectively binds to intracellular lipid droplets. VAT, but not spleen, T_{regs} readily took up lipids, especially in response to Pio (Fig. 4d). This process was PPARγ-dependent as the Pio-induced increase in CD36 expression and Nile red staining were both greatly dampened in T_{reg}-*Pparg* mutant mice (Suppl. Fig. S7e and f). Thus, Pio accentuates the accumulation and phenotype of fat T_{regs} in epididymal fat depots of obese mice.

The striking increase in the representation of and alterations in the phenotype of VAT T_{regs} provoked by Pio treatment of obese mice raised the question of whether this population contributes to the insulin-sensitizing effect of Pio. In analogy to the human context, we compared immunologic and metabolic parameters in obese (HFD-fed) *Pparg* wt and T_{reg}-*Pparg* mut mice as a function of Pio co-treatment. As anticipated, the VAT T_{reg} population of wt animals fed a HFD was quite low, and it increased substantially when Pio was included in the diet (Fig 4e). Also as expected, the representation of VAT T_{regs} in mutant animals on HFD was similar to that of their wt counterparts: HFD in and of itself results in death and/or evacuation of typical VAT T_{regs}, so abrogation of PPARγ expression in this context has no further impact. Pio could not expand VAT T_{regs} in the mutant (Fig 4e). Pio had differential effects on conventional adipose-tissue monocyte/macrophage populations in HFD-fed mutant mice: pro-inflammatory macrophages ($CD11b^+CD11c^+F4/80^+$) were diminished, though not to the degree seen in wt littermates (Suppl. Fig. S8a); in contrast, pro-inflammatory monocytes ($CD11b^+Ly6c^{hi}$) did not undergo their usual reduction (Suppl. Fig. S8b, left); while anti-inflammatory monocytes ($CD11b^+Ly6c^{low}$) uncharacteristically declined (Fig. S8b, right). Pio treatment of obese mutant mice was less effective than treatment of their wt counterparts at normalizing systemic metabolic parameters: homeostatic model assessment of insulin resistance (HOMA-IR) (Fig. 4f), glucose and insulin tolerance (Fig. 4g and Suppl. Fig. S8c), and phosphorylated (p)AKT levels in multiple organs (Suppl. Fig. S8d). At least some of the muted metabolic response to Pio reflected events in VAT, evidenced by the lack of normalization of pAKT values at that site. The Pio treatment clearly worked, however, as we did see in both wt and mutant drug-

treated HFD-fed mice the expected increase in epididymal fat-pad weight (Suppl. Fig. S9a), though not in total body weight (not shown); a coupled decrease in adipocyte numbers and increase in adipocyte size (Suppl. Fig. S9b and c); and increased levels of serum adiponectin and *Adipoq* transcripts (Suppl. Fig. S9d). Leptin (*Lep*) transcript levels were unchanged in both wt and HFD-fed individuals (Suppl. Fig. S9e), as anticipated [7].

The main conclusion from our results is that PPARγ is a major orchestrator of the unique properties of VAT T_{regs}. This nuclear receptor collaborates with Foxp3 to impose on naïve $CD4^+$ T cells the transcriptional signature characteristic of VAT T_{regs}. Interestingly, both PPARγ isoforms can promote the fat T_{reg} up-signature in conjunction with Foxp3, but only isoform 1 drives the down-signature. This constitutes a rare dysjunction in the activities of the two PPARγ isoforms, which differ only an additional 30 amino acids at the N-terminus of PPARγ2. Experimental manipulation of PPARγ specifically in $Foxp3^+$ cells had a clear and precise impact on the accumulation and phenotype of T_{regs} in epididymal fat depots. A newly discovered property was that VAT, but not lymphoid-tissue, T_{regs} can take up lipids, an intriguing adaptation to the tissular environment, not shared by conventional T cells residing at the same site. It remains to be determined whether this feature promotes T_{reg} survival or effector functions, or whether it is an epiphenomenon.

Our data also indicate that PPARγ expressed by T_{regs} contributes substantially to the insulin-sensitizing activity of Pio. It was initially assumed, given this transcription factor's role in fat-cell differentiation, that TZD drugs improve metabolic parameters in obese individuals by activating PPARγ in adipocytes. While this notion has received experimental support [8], other studies have argued for the importance of PPARγ expression in macrophages [9, 10], muscle [11] and the central nervous system [12, 13]. On first consideration, it seems difficult to explain the need for PPARγ across such a broad range of cell-types, but several points should be kept in mind. First, TZD drugs may impact several processes upstream of insulin resistance, e.g. ingestive behavior, adipocity and inflammation; PPARγ-driven programs in different cell-types may influence these processes differentially. Secondly, abrogating PPARγ expression in different cell-types appears to have organ-specific effects on insulin resistance [11–13]. And third, there is increasing appreciation that the gene promoters used to generate transgenic mouse lines with cell-type-specific ablation of PPARγ can be "leaky." Delineating the cell-type(s) critical for Pio's protective effect on metabolic disorders is imperative given current concerns over the side-effects of the TZD class of compounds and the resultant search for alternative drugs [14].

Lastly, our results provide proof-of-principle that it is possible to target a designated population of T_{regs} for a particular therapeutic goal. The emerging notion that the $Foxp3^+CD4^+$ T_{reg} compartment includes a number of sub-types with distinct phenotypes, localizations and effector functions [15] has evoked the exciting possibility of developing strategies to precisely expand or contract disease-relevant T_{regs}, leaving the bulk of the compartment intact to maintain immune homeostasis.

METHODS SUMMARY

Source and maintenance of mice are described in Methods. Experimentals and controls were always littermate-matched males (eg, $Pparg^{fl/fl}$-$FoxP3^{YFP\text{-}Cre}$ and $Pparg^{wt}$-$FoxP3^{YFP\text{-}Cre}$). HFD and NC animals were fed a diet containing 60 kcal% and 10 kcal% fat, respectively. Mice on HFD+Pio were fed the above-described diet mixed with Pio at a concentration of 100 mg per kg of food. Metabolic studies were performed on mice fed HFD +/− Pio for 12 weeks. For GTTs, glucose (2.0g per kg body-weight) was administered by ip injection after an overnight fast. For ITTs, insulin (0.75 units) was administered by ip injection after 4 hours of fasting.

$CD4^+CD25^-$ T cells were activated for 48-hours with anti-CD3/CD28 antibody-coated beads plus recombinant human IL-2 before retroviral transduction and cultured for 72 hours after transduction. In selected experiments, 24 hours after infection, transduced cells were treated with 1μM Pio, Rosi or GW1929, or with vehicle (DMSO) for 48 hours before sorting.

For T cell analysis, cells were stained with anti-CD45, -CD3, -CD4, -CD8, -CD25-and sometimes anti-CD36, fixed, permeabilized and intracellularly stained for Foxp3 and Gata-3. For intracellular lipids, cells were stained with anti-CD3, -CD4 and Nile red (1μg/mL). RNA from double-sorted cells was prepared for microarray analysis [2], and hybridized to GeneChip Mouse Genome M1.0 ST arrays (Affymetrix).

Supplementary Material

Refer to Web version on PubMed Central for supplementary material.

Acknowledgments

We thank Drs. A. Rudensky, F. Gonzalez, R. Kahn, B. Spiegelman and D. Vignali for providing materials; K. Hattori, M. Davenport, J. LaVecchio, G. Buruzala, J. Ericson, K. Leatherbee and S. Davis for technical assistance; Drs. A. Ergun, A. Morton and J. Shu for experimental help; and Drs. M. Wilson and J. Hill for discussions. Supported by grants from the NIH (DK092541) and Ellison Foundation (Boston) to DM and CB, Dana Foundation to DM and SS; the American Diabetes Association (RA 110BS97) to JL and NIH (DK51729) to SS; as well as by core facilities of the Joslin Diabetes Center (P30DK36836). MF received a postdoctoral fellowship from the King Trust.

References

1. Osborn O, Olefsky JM. The cellular and signaling networks linking the immune system and metabolism in disease. Nat Med. 2012; 18:363–374. [PubMed: 22395709]
2. Feuerer M, et al. Lean, but not obese, fat is enriched for a unique population of regulatory T cells that affect metabolic parameters. Nat Med. 2009; 15:930–939. [PubMed: 19633656]
3. Winer S, et al. Normalization of obesity-associated insulin resistance through immunotherapy. Nat Med. 2009; 15:921–929. [PubMed: 19633657]
4. Ilan Y, et al. Induction of regulatory T cells decreases adipose inflammation and alleviates insulin resistance in ob/ob mice. Proc Natl Acad Sci U S A. 2010; 107:9765–9770. [PubMed: 20445103]
5. Tontonoz P, Spiegelman BM. Fat and beyond: the diverse biology of PPARgamma. Annu Rev Biochem. 2008; 77:289–312. [PubMed: 18518822]
6. Tontonoz P, et al. PPARgamma promotes monocyte/macrophage differentiation and uptake of oxidized LDL. Cell. 1998; 93:241–252. [PubMed: 9568716]
7. Miyazaki Y, et al. Effect of pioglitazone on circulating adipocytokine levels and insulin sensitivity in type 2 diabetic patients. J Clin Endocrinol Metab. 2004; 89:4312–4319. [PubMed: 15356026]
8. Sugii S, et al. PPARgamma activation in adipocytes is sufficient for systemic insulin sensitization. Proc Natl Acad Sci U S A. 2009; 106:22504–22509. [PubMed: 20018750]
9. Hevener AL, et al. Macrophage PPAR gamma is required for normal skeletal muscle and hepatic insulin sensitivity and full antidiabetic effects of thiazolidinediones. J Clin Invest. 2007; 117:1658–1669. [PubMed: 17525798]
10. Odegaard JI, et al. Macrophage-specific PPARgamma controls alternative activation and improves insulin resistance. Nature. 2007; 447:1116–1120. [PubMed: 17515919]
11. Hevener AL, et al. Muscle-specific Pparg deletion causes insulin resistance. Nat Med. 2003; 9:1491–1497. [PubMed: 14625542]
12. Ryan KK, et al. A role for central nervous system PPAR-gamma in the regulation of energy balance. Nat Med. 2011; 17:623–626. [PubMed: 21532595]
13. Lu M, et al. Brain PPAR-gamma promotes obesity and is required for the insulin-sensitizing effect of thiazolidinediones. Nat Med. 2011; 17:618–622. [PubMed: 21532596]

14. Olefsky JM, Lazar MA, Scherer PE. Antidiabetes wars: a new hope. Nat Med. 2010; 16:972–973.
15. Josefowicz SZ, Lu LF, Rudensky AY. Regulatory T Cells: Mechanisms of Differentiation and Function. Annu Rev Immunol. 2012

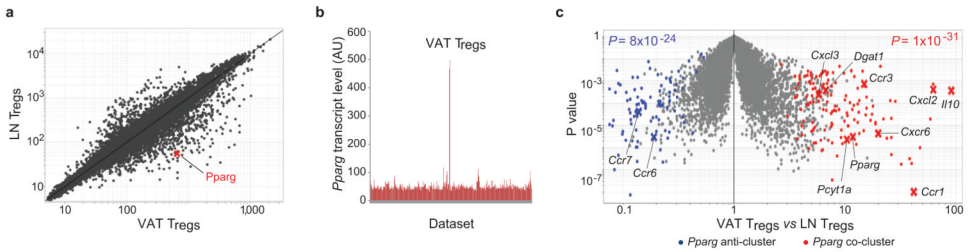

Fig. 1. Transcripts directly or inversely correlated with *Pparg* expression in VAT T_{regs}

(a) Microarray analysis. Normalized expression values for transcripts isolated from T_{regs} from epididymal fat versus LN of 30-week-old retired-breeder B6 males (in triplicate). **(b)** Expression of *Pparg* in a library of microarray datasets from diverse T cell populations: different subsets, activation statuses, or location. **(c)** A volcano plot comparing gene expression in VAT and LN T_{regs} of NC-fed B6 mice. The *Pparg* co- and anti-cluster transcripts defined in Suppl. Fig. 1b are superimposed in red and blue, respectively. Some of the characteristic of VAT T_{reg} genes are indicated. *P* values from a chi-square test.

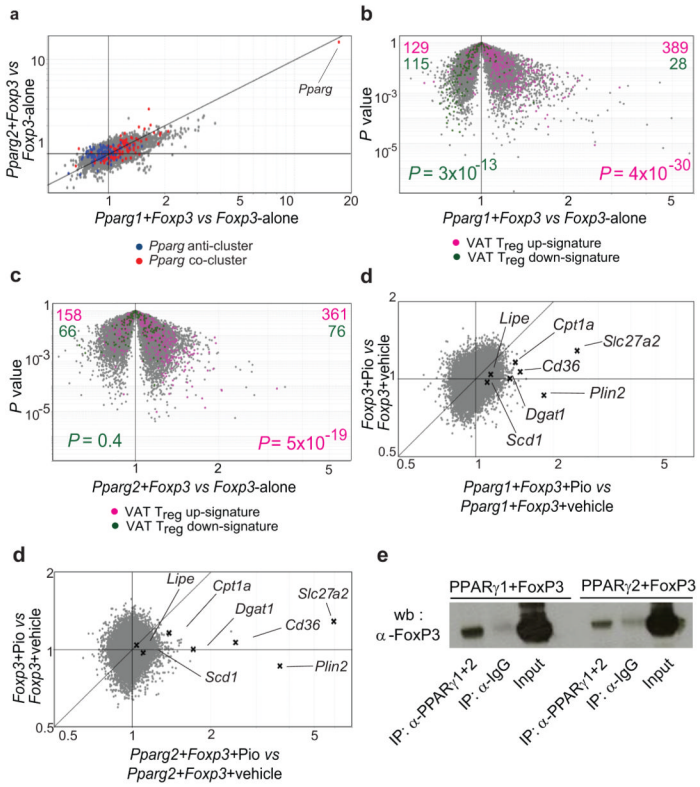

Fig. 2. Cooperation between PPARγ and Foxp3

Naive CD4^{+}CD25^{-} T cells were stimulated *ex vivo* and transduced with retroviruses encoding *Foxp3* (MSCV IRES-GFP) plus *Pparg1* or *Pparg2* (both MSCV IRES-Thy1.1). Cells were sorted for green-fluorescent protein (GFP) and/or Thy1.1 positivity before RNA processing. **(a)** An FC/FC plot comparing gene-expression values for double-transductants expressing *Pparg1* and *Foxp3* versus single-transductants expressing *Foxp3* only (x-axis) vis-á-vis double-transductants expressing *Pparg2* and *Foxp3* versus single-transductants expressing *Foxp3* (y-axis). *Pparg* co-cluster and anti-cluster genes are superimposed in red and blue, respectively. **(b, c)** Genes from the VAT T_{reg} up- and down-signature highlighted in pink and green, respectively, on a volcano plot comparing *P* value versus FC for probes from double-transductants expressing *Foxp3* and *Pparg1* or *Foxp3* and *Pparg2* versus single-transductants expressing *Foxp3* alone. The VAT T_{reg} up- and down-signatures were defined as described in Methods. *P* values from a chi-square test. **(d, e)** 24 hours after transduction of naïve CD4^{+} T cells, double-transductant (*Pparg1+Foxp3* or *Pparg2+Foxp3*) or single-transductant (*Foxp3* alone) cultures were treated with Pio (1μM) for 48 hours. FC/FC plots comparing gene expression values of Pio-treated versus vehicle-treated double-transductants expressing *Pparg1* or *Pparg2* plus *Foxp3* (x axis) vis-á-vis Pio-treated versus vehicle-treated single-transductants expressing *Foxp3* alone (y axis). Some genes involved in lipid metabolism are indicated. Mean expression values calculated from three independent experiments. **(f)** Association of Foxp3 with PPARγ determined by co-immunoprecipitation. Anti-PPARγ1+2 antibody was used to immunoprecipitate PPARγ1 or PPARγ2 from nuclear lysates of HEK293 cells co-transduced with *Foxp3* and *Pparg1* or *Pparg2*. Immunoblots were probed with anti-Foxp3.

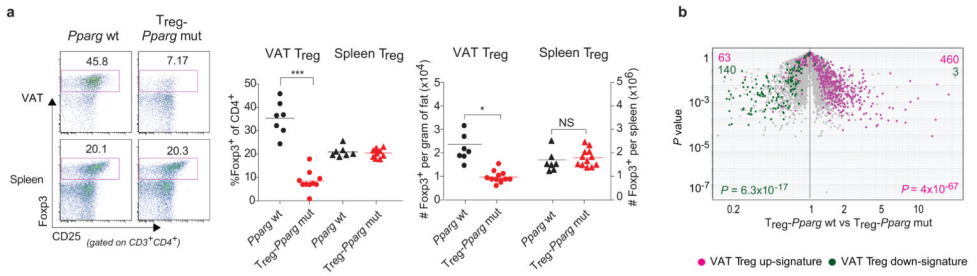

Fig. 3. *In vivo* effects of abrogating PPARγ expression specifically in T_{regs}

(a) T_{reg} representation. Cells were isolated from the spleen or stromovascular fraction (SVF) of epididymal fat (epi-fat) of 25-week-old mice lacking PPARγ specifically in T_{regs} (T_{reg}-*pparg* mut) or littermate controls (*Pparg* wt). T_{regs} are defined as $CD45^+CD3^+CD4^+Foxp3^+$. Left, representative dot plots (of at least 3 experiments); center, summary data (for fraction of $CD4^+$ cells); right, numbers per gram of tissue. Dot plot numbers indicate the percentage of cells in that gate for that particular experiment. *P* values according to the Student's T test: **P*<0.05, ***P*<0.01, ****P*< 0.001; NS=not significant. Error bars represent the mean ± SD. **(b)** Expression of VAT T_{reg} signature genes in T_{reg}-*Pparg* mut mice. A volcano plot comparing *P* value versus FC for probes from wt versus mutant VAT T_{regs}. Genes from the VAT T_{reg} up- and down-signature are highlighted in pink and green, respectively. *P* determined by the chi-square test.

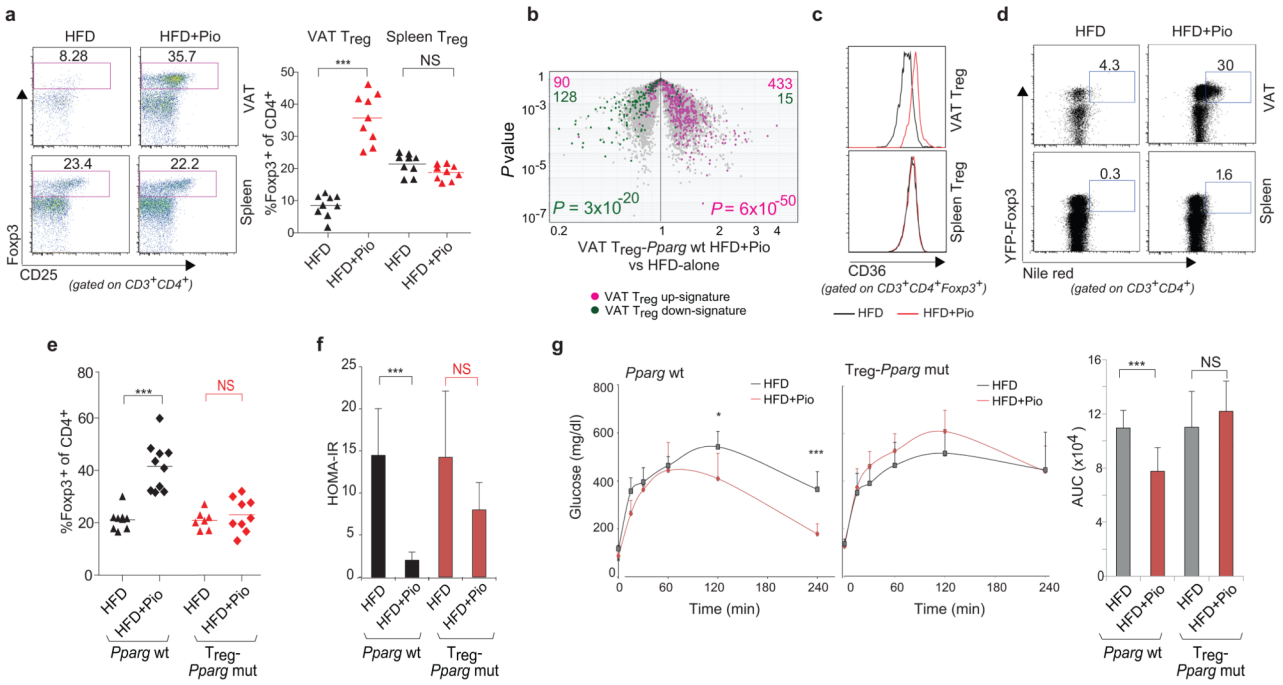

Fig. 4. Pio promotion of epididymal fat T_{reg} numbers and phenotype

At 9 weeks of age, *Pparg* wt and T_{reg}-*Pparg* mut mice were fed HFD +/− Pio for 13 weeks. Cells from the spleen and epididymal fat SVF were stained and analyzed by flow cytometry. Numbers on dot plots indicate the percentage of cells in that gate for that particular experiment (representative of ≥3 experiments). **(a)** T_{regs} from *Pparg* wt mice on HFD +/− Pio. Left, representative dot plots; right, summary data. **(b)** Expression of VAT T_{reg} signature genes in *Pparg* wt mice on HFD+/−Pio. A volcano plot comparing *P* value versus FC for probes from VAT T_{regs} isolated from *Pparg* wt mice on HFD+Pio versus HFD alone. Genes from the VAT T_{reg} up- and down-signature are highlighted in pink and green, respectively. *P* determined by the chi-square test. **(c)** MFI of CD36 expression by T_{regs}. ΔMFI indicates, for gated $CD3^+CD4^+Foxp3^+$ cells, the difference in CD36 expression for HFD-fed mice +/− Pio treatment. Epi-fat ΔMFI = 3828±1362 (**P*=0.039); spleen ΔMFI = −182±597 (NS). **(d)** Cells were isolated from the spleen or epi-fat SVF of B6.*Foxp3-(YFP −)Cre* mice kept on HFD+/−Pio for 13 weeks, and stained for CD3, CD4 and Nile red. **P*=0.01. **(e)** T_{reg} fraction. Cells from spleen or epi-fat SVF were stained and analyzed by flow cytometry. **(f)** Insulin sensitivity. Mice were assessed for blood fasting-glucose and fasting-insulin levels. These values were used to calculate the HOMA-IR. (g) Glucose tolerance. Left: intraperitoneal GTT on wt mice. Center: GTT on mutant mice. Right: area under the curve (AUC) calculations. *n*=13–14 mice per group. *P* values calculated using the Student's T test. Unless otherwise specified: **P*<0.05, ***P*<0.01, ****P*< 0.001; NS=not significant. Error bars represent the mean ± SD for immunological parameters, mean ± SE for metabolic parameters, as is standard practice in the respective fields.